Characterization of the Protonation and Hydrogen Bonding State of the Histidine Residues in IIA^{mtl}, a Domain of the Phosphoenolpyruvate-Dependent Mannitol-Specific Transport Protein†

Alard A. Van Dijk,* Ruud M. Scheek, Klaas Dijkstra, Gea K. Wolters, and George T. Robillard

Department of Biochemistry and the Institute BIOSON, State University of Groningen, Nijenborgh 4, 9747 AG Groningen, The Netherlands

Received March 3, 1992; Revised Manuscript Received June 16, 1992

ABSTRACT: The A domain of the mannitol-specific EII, IIA^{mtl}, was subcloned and proven to be functional in the isolated form (Van Weeghel et al., 1991). It contains a histidine phosphorylation site, the first of two phosphorylation sites in the parent protein. In this paper, we describe the characterization of the three histidine residues in IIA^{mtl} with respect to their protonation and hydrogen bonding state, using $^1H\{^{15}N\}$ heteronuclear NMR techniques and protein selectively enriched with [$\delta1,\epsilon2$-^{15}N]histidine. The active site residue has a low pK_a (<5.8) and shows no hydrogen bond interactions. The proton in the neutral ring is located at the N$\epsilon2$ position, which also proved to be the site of phosphorylation. The phosphorylation raises the pK_a of the active site histidine considerably but does not change the hydrogen bond situation. The other two histidine residues, one of which is probably located on the surface of the protein, were also characterized. Both show hydrogen bond interactions in the unphosphorylated protein, but these are disturbed by the phosphorylation process. These observations, combined with small changes in pK_a and titration behavior, indicate that the IIA^{mtl} changes its conformation upon phosphorylation.

EII^{mtl} [1] is the membrane component of the mannitol-specific phosphoenolpyruvate- (PEP-) dependent phosphotransferase system (PTS)[2] in *Escherichia coli*. It takes care of the transport of mannitol across the inner membrane and its concomitant phosphorylation. The phosphoryl group in this process is donated initially by PEP and is shuttled to the EII^{mtl} via EI and HPr. Phospho-HPr phosphorylates a histidine residue (His554) of EII^{mtl}; the phosphoryl group is then transferred to a cysteine residue, Cys384, and finally to the incoming sugar. (Pas & Robillard, 1988; Pas et al., 1988, 1991). EII^{mtl} consists of three domains, A, B, and C. The A and B domain are cytoplasmic and contain the phosphorylation sites, the C domain is located in the membrane. The A domain, IIA^{mtl}, containing the His554 phosphorylation site was recently subcloned, overexpressed, and purified by Van Weeghel et al. (1991). The separated domain is able to perform the same tasks as when integrated in the parent enzyme. The general characterization of IIA^{mtl} and its interaction with HPr will be treated in a separate study. This paper treats the hydrogen bond structure at the three histidine residues in IIA^{mtl} and the changes that take place upon phosphorylation of the protein.

MATERIALS AND METHODS

Bacterial Strains and Growth. *Escherichia coli* JC411 (*his*$^-$, *arg*$^-$, *leu*$^-$, *met*$^-$) was transformed with the plasmid pMcCI, described by Van Weeghel et al. (1991) using standard procedures. The strain was grown at 37 °C on the mineral medium described by Van Dijk et al. (1990), containing $\delta1,\epsilon2$-^{15}N-labeled histidine (20 μg/mL) as the sole histidine source and chloramphenicol (20 μg/mL) instead of ampicillin as antibiotic. Cells were allowed to grow for 2–3 days after which they were harvested by centrifugation (10000*g*, 5 min, 4 °C).

Purification of IIA^{mtl}. IIA^{mtl} was purified at 4 °C by a procedure slightly different from the one described by Van Weeghel et al. (1991). Cells were resuspended in buffer 1 (20 mM Tris-HCl (pH 7.6), 1 mM DTT, 1 mM EDTA, 1 mM NaN_3; 10 mL/g wet weight). DNase and RNase (0.03 mg/mL) were added, and the cells were disrupted in a French press (10 000 psi). Cell debris was removed by centrifugation (48000*g*, 2 h) and the supernatant was collected. The pellet was resuspended in buffer 1 (2 mL/g wet weight) and recentrifuged as described. The supernatant was collected and added to the first supernatant. The resulting solution was dialyzed against 2 L of buffer 2 (20 mM Tris-HCl (pH 9.5), 1 mM DTT, 150 mM NaCl, 1 mM NaN_3). The dialyzed solution was loaded on a Q-Sepharose column (2 × 20 cm; 0.7 mL/min), equilibrated in buffer 2. After the column was washed with at least an additional 200 mL of buffer 2, the IIA^{mtl} was eluted with a linear NaCl gradient (2 × 150 mL; 150–300 mM NaCl). Fractions were collected and assayed for IIA^{mtl} activity with the IIA^{mtl} complementation assay (Van Weeghel et al., 1991). IIA^{mtl}-containing fractions were pooled and dialyzed overnight against 3 L of buffer 3 (10 mM Tris-HCl (pH 7.6), 1 mM NaN_3) after which the solution was concentrated to 30 mL on an Amicon ultrafiltration apparatus, using a FILTRON Omega 3 filter. The concentrated solution was loaded on a Sephadex G75 column (5 × 70 cm, 2 mL/min) equilibrated in buffer 3. Fractions were collected and

† This research was supported by the Netherlands Foundation for Chemical Research (SON) with financial aid from the Netherlands Organization for Scientific Research (NWO). The ^{15}N-labeled histidine used in this study was provided by the National Stable Isotope Resource at Los Alamos, NM.

* Address correspondence to this author at the following present address: Gesellschaft für Biotechnologiche Forschung (GBF), Mascheroder Weg 1, D-3300 Braunschweig, Germany.

[1] Abbreviations: EI, enzyme I; glc, glucose; HMQC, heteronuclear multiple quantum coherence; lac, lactose; man, mannose; mtl, mannitol; PEP, phosphoenolpyruvate; PTS, phosphoenolpyruvate-dependent phosphotransferase system; TPPI, time-proportional phase incrementation; xtl, xylitol.

[2] Throughout this paper we use the nomenclature for the PTS that has been suggested by Saier and Reizer (1991).

0006-2960/92/0431-9063$03.00/0

assayed for IIA^{mtl} activity as described. The IIA^{mtl}-containing fractions were pooled and subjected to polyacrylamide gel electrophoresis. The protein migrated as a single homogeneous band.

Other Enzyme Purifications and Determination of Enzyme Concentration. HPr was isolated as described by Van Dijk et al. (1991) and EI was isolated according to Robillard et al. (1979). Enzyme concentrations were determined by the pyruvate burst method, described by Robillard and Blaauw (1987).

Gel Electrophoresis. Polyacrylamide gel electrophoresis was performed as described by Laemmli (1970) with 12.5% acrylamide gels. Gels were stained by Coomassie staining or by silver staining (Wray et al., 1981).

Preparation of IIA^{mtl} and $PIIA^{mtl}$ Samples for NMR Measurements. IIA^{mtl} (2–4 mM) solutions were brought to the appropriate pH by dialyzing 0.5 mL of the solution against 20 mL of KP_i buffer (50 mM in D_2O, 2 mM EDTA, 1 mM NaN_3) at the desired pH. The pH was measured before and after each series of spectra, and values agreed to within 0.05 unit. $PIIA^{mtl}$ was generated in situ in the NMR tube by first dialyzing the IIA^{mtl} solution against 5 mL of D_2O buffer containing 50 mM KP_i, 500 mM PEP, 5 mM $MgCl_2$, 5 mM EDTA, 1 mM DTT, and 1 mM NaN_3. After 2 h of dialysis, 50 μL of a solution containing EI (250 μM) and HPr (360 μM) was added, resulting in the rapid phosphorylation of IIA^{mtl}. NMR measurements were started 10 min after the addition of EI and HPr. The presence of characteristic PEP proton resonances in the NMR spectra of $PIIA^{mtl}$ confirmed the presence of excess PEP throughout the NMR measurement.

NMR Measurements. All NMR spectra were recorded at 26 °C with a VARIAN VXR500 NMR spectrometer, operating at a ^1H frequency of 500 MHz and equipped with a SUN 3/160 computer. $^1H\{^{15}N\}$ heteronuclear multiple quantum coherence (HMQC) spectra were recorded using the pulse sequence described by Bendall et al. (1983). Spectra were recorded with $\omega1(^{15}N)$ = 10 000 Hz and $\omega2(^1H)$ = 6666 Hz, with 256 increments in $\omega1$. For each $t1$ value 128, 192, or 256 transients were recorded, the number of scans depending on the experiment. The acquisition time in $t2$ was 0.154 s using 2048 data points. The J-value was set to 30 Hz, which in pilot experiments proved to give the best signal to noise ratio. During acquisition, the ^{15}N was decoupled using a broadband WALTZ decoupling. Spectra were recorded using time-proportional phase incrementation (TPPI) to allow for the discrimination between positive and negative frequencies in $\omega1$ and $\omega2$. Spectra with different φ_1 were stored separately to allow for small corrections in phase and amplitude after Fourier transformation in $t2$ (^1H). Data processing was performed on a Convex C1-XP computer, using the program SNARF developed in our lab by F. van Hoesel. FIDs were Fourier transformed using a Lorentzian to Gaussian filter in both time domains and a Hanning window in $t1$ (^{15}N) and sometimes in $t2$ (^1H). A simple baseline correction was performed in $t1$ after Fourier transformation. ^1H chemical shifts are referenced to internal 2,2-dimethyl-2-silapentane-1-sulfonate (DSS); ^{15}N chemical shifts (absolute value) are relative to external 1 M $H^{15}NO_3$.

Appearance and Interpretation of $^1H\{^{15}N\}$ HMQC Spectra. ^{15}N NMR provides insight into the hydrogen bond structure at imidazole ring systems. On the basis of a series of model studies, Bachovchin (1986) proposed a division of imidazole nitrogens into three types, α, α^+, and β. They have characteristic chemical shifts, reflecting the protonation state of the individual nitrogens and the entire ring (see Table I).

Table I: ^{15}N Chemical Shift Positions[a] of Imidazole Nitrogens in the NMR Spectrum, As Described by Bachovchin (1986)

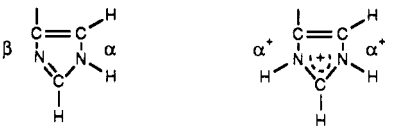

^{15}N type	chemical shift position (ppm)	maximal H-bond effect (ppm)
α	210	−10
α^+	201	−10
β	128	+10

[a] Chemical shift positions are relative to external 1 M $H^{15}NO_3$ (absolute values).

Hydrogen bond interactions at the imidazole nitrogens also influnece the ^{15}N chemical shift positions. The α-type and α^+-type nuclei can function as H-donors; the β-type can function as H-acceptors using their lone electron pair. These interactions result in small but distinct changes in the resonance positions of the imidazole nitrogens, the α or α^+ moving maximally 10 ppm downfield, the β moving maximally 10 ppm upfield, (Bachovchin, 1986). These effects are also given in Table I. This classification of ^{15}N NMR chemical shifts has been used to characterize the protonation and hydrogen bonding state of histidine residues in a number of proteins (Bachovchin & Roberts, 1978; Bachovchin, 1985, 1986; Van Dijk et al., 1990). In this study, $^1H\{^{15}N\}$ HMQC spectra of the histidine residues in IIA^{mtl} were recorded. The $^2J_{NH}$ couplings of the Nδ1 and Nϵ2 nuclei to the C2 and C4 protons allow one to determine the resonance frequencies of all four nuclei in a single HMQC spectrum. The protons that are directly attached to the nitrogens are not observed because they exchange with water too quickly to be detected. When dealing with a neutral imidazole ring system, two extreme situations can occur. The first is when the hydrogen is firmly located on one of the nitrogen nuclei, resulting in an imidazole ring with an α-type and a β-type nitrogen. One then observes a triangle of cross-peaks in the HMQC spectrum as in Figure 1a with the C2H proton reporting two ^{15}N frequencies, one at 210 ppm corresponding to an α-type nitrogen and one at 128 ppm corresponding to a β-type nitrogen. The C4H reports only one nitrogen frequency corresponding to a β-type nitrogen. The coupling between the Nδ1 and C4H is too small (1–2 Hz) to result in an observable cross-peak. The cross-peak pattern enables the unambiguous assignment of the nitrogen and proton frequencies to specific nuclei and at the same time specifies which nitrogen is protonated. In Figure 1a, the Nδ1 is protonated; if the Nϵ2 had been protonated, the C4H cross-peak would have been located at an ^{15}N frequency of 210 ppm.

The second extreme occurs when the proton is not located on one of the nitrogens but exchanges rapidly between the two. If the proton shows no prefeence for the Nδ1 or Nϵ2, the nitrogens are magnetically equivalent and resonate at the same frequency of 169 ppm, the average between the α and β resonance position, resulting in a HMQC spectrum with two cross-peaks as in Figure 1b. Intermediate situations exist, for example, when there is a slow tautomerization as shown in Figure 1c. This results in four cross-peaks instead of three. Both the Nδ1 and the Nϵ2 have α character part of the time and β character the rest of the time. When the Nδ1 has α character, it resonates at the α position of 210 ppm; when it has β character it resonates at the β position of 128 ppm. The same holds for the Nϵ2 nucleus. Consequently, both the C2H

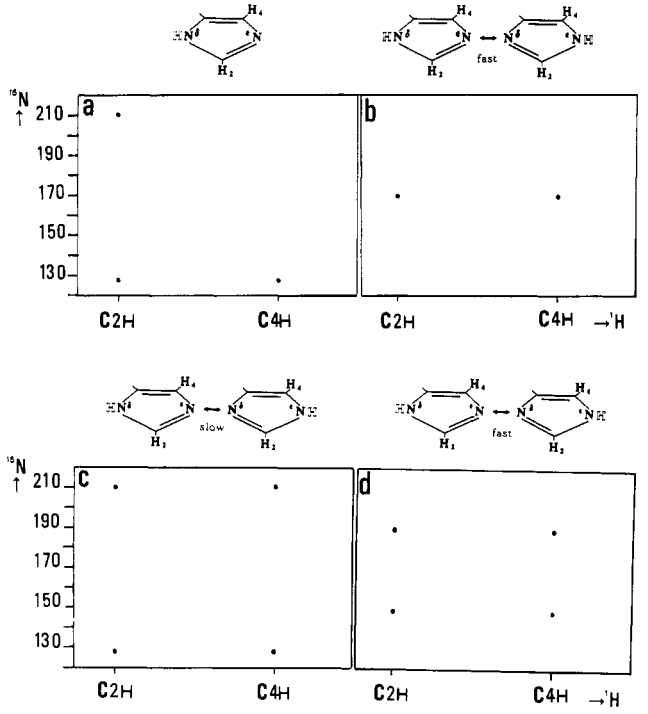

FIGURE 1: Model H{^{15}N} HMQC spectra showing the cross-peak patterns for imidazole rings with different tautomerization states. (a) The proton is localized at the Nδ1 position. (b) The proton exchanges between Nδ1 and Nε2 in a fast tautomerization process. (c) The proton exchanges between Nδ1 and Nε2 in a slow tautomerization. (d) A fast tautomerization situation is represented, but one in which the proton has a preference for one of the N positions. The nuclei observed in the spectra are given in bold type; the proton directly attached to the nitrogen is not observed and is given in an open notation. We will use this notation throughout the paper.

and C4H report two nitrogen frequencies, an α-type and a β-type, corresponding to the two different tautomers. When the tautomeric equilibrium is fast but the proton prefers one of the nitrogens, the HMQC spectrum looks like Figure 1d. The explanation is the same as for Figure 1c, except that the Nδ1 and the Nε2 now show a signal at a position that depends on their relative α-type and β-type character. For instance, when the Nδ1 has 75% α character, it will resonate at 128 ppm + 0.75 × 82 ppm = 189.5 ppm where 128 is the β position and 82 is the difference between the α and β position; the Nε2 then resonates at 148.5 ppm. The magnitude of the rate constants in the tautomeric equilibrium are decisive for the spectral appearance of the resonances in the HMQC spectrum. The fast and slow exchange situations have been discussed; with intermediate exchange the HMQC spectrum may show no cross-peaks at all due to exchange broadening in the ^{1}H and/or ^{15}N domain.

RESULTS

^{1}H{^{15}N} HMQC spectra of [δ1,ε2-^{15}N]histidine-labeled IIA^{mtl} recorded at several pH values provided the data for the titration curves for the ^{1}H and ^{15}N nuclei in the histidine imidazole rings. The data for the ^{1}H titration curves were extended with 1D ^{1}H NMR measurements at several pH values using a nonlabeled IIA^{mtl} preparation.

Relaxation Behavior of the Histidine Resonances

Figure 2 shows the HMQC spectrum for IIA^{mtl} at pH = 7.5. The three histidine spin systems are indicated by the lines drawn. The HisB spin system shows fast tautomerization as is evident from its nitrogen chemical shift positions (184 ppm and 191 ppm for Nδ1 and Nε2, respectively); it is comparable to the situation depicted in the model spectrum in Figure 1d. The other two histidine spin systems clearly show a proton localization at the Nδ1 (HisC) or the Nε2 (HisA). In addition to different tautomerization states, the histidines also show very different relaxation behavior. This is evidenced by the intensity of the signals of the resonances in the HMQC spectrum. The resonances of HisA are the weakest in the spectrum; the ones of HisC are stronger but they are still much less intense than the signals of HisB. The intensity of a cross-peak in the HMQC spectrum is defined by two processes, the buildup of the signal via the *J*-coupling and its decay via relaxation. The intensity of the cross-peaks in the absence of any relaxation is described by eq 1, using

$$M(t) = -I_y \sin^2(2\pi J\tau) \cos(\omega_N t) \quad (1)$$

the product operator notation of Soerensen et al. (1983). $M(t)$ is the observed magnetization in the xy plane, I_y is the product operator representing the in-phase y magnetization of the ^{15}N nucleus, J is the coupling constant between the nitrogen and proton nucleus, τ is the delay time, ω_N is the Larmor frequency of the nitrogen nucleus, and t is the evolution time in the ^{15}N domain. Equation 1 shows that the magnetization is dependent on several parameters which are, however, essentially the same for all the histidine residues in IIA^{mtl}. The magnitude of the *J*-coupling constant varies slightly with the protonation state of the imidazole ring (Blomberg et al., 1977). We will show later that the protonation state of the three histidines in IIA^{mtl} is not the same at the pH at which Figure 2 was recorded. This will affect the the signal intensities of the cross-peaks to some extent. However, it cannot account for the huge differences in signal intensities, observed in Figure 2. These must arise from differences in relaxation rates of the histidine residues, provided that nuclei are not involved in intermediate exchange processes. The more intense the cross-peaks, the slower the relaxation. The slow relaxation of the HisB indicates a high degree of mobility characteristic of side chains situated on the outside of the protein. The other two histidine residues are probably located more to the interior of the molecule.

Evaluation of the Recorded Titration Curves

^{1}H Titration Curves. The ^{1}H titration curves for the three histidine residues in IIA^{mtl} are given in Figure 3. The data are taken from 1D ^{1}H measurements and ^{1}H{^{15}N} HMQC spectra. Assignment of the resonances was done by using the HMQC spectra, as has been discussed. The data points for each resonance were fitted to eq 2, using a least-squares fitting

$$\delta_{obs} = \delta_a + [x/(x + K_a)](\delta_b - \delta_a) \quad (2)$$

procedure. K_a is the acid dissociation constant, δ_{obs} is the observed chemical shift position. δ_a and δ_b are the chemical shift positions of the protons in the fully protonated and deprotonated imidazole ring respectively, and x is the H^+ concentration (moles per liter). The solid lines in the figure result from the fit. The results of the analysis are summarized in Table II. The pK_a values for HisA could not be determined because when the HisA starts titrating at pH = 5.8, its resonances broaden and become undetectable; at lower pH values the protein also rapidly precipitates. HisB shows normal titration behavior but HisC is peculiar in that its C4H shows almost no titration behavior at all (Table II). It titrates only 0.04 ppm whereas 0.4 ppm is normal for such a proton.

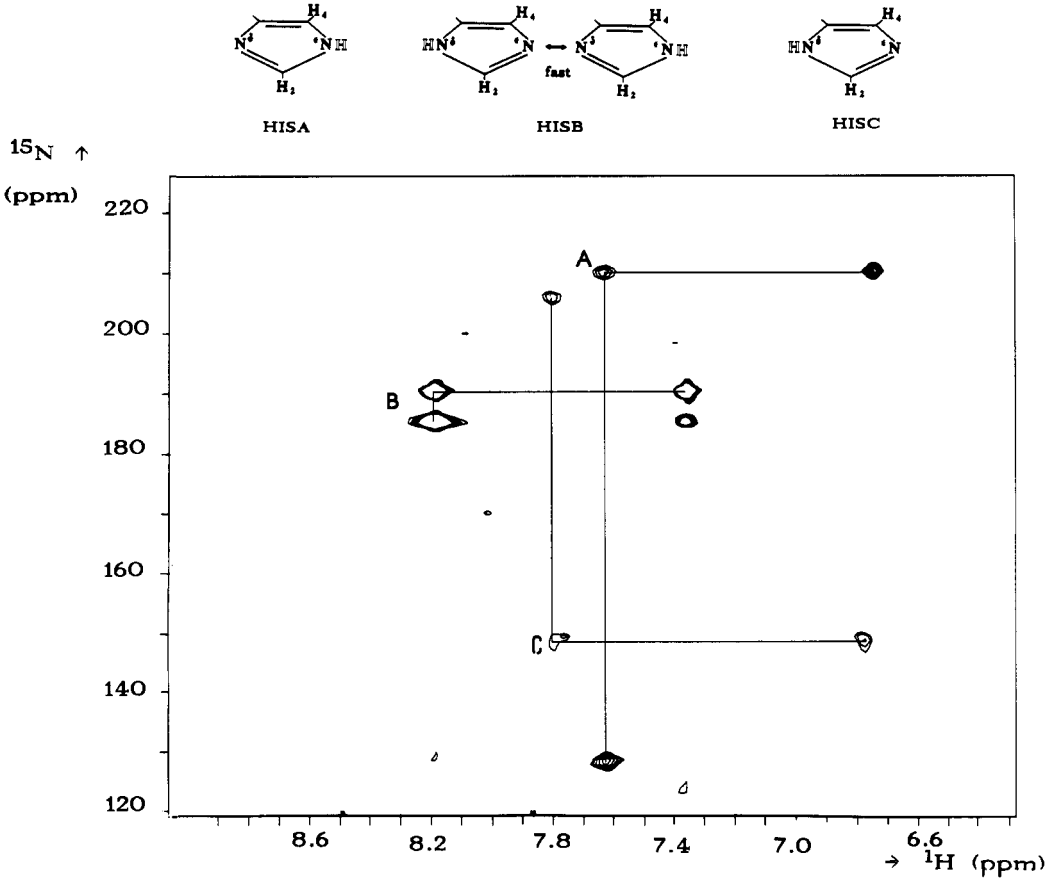

FIGURE 2: $^{1}H\{^{15}N\}$ HMQC spectrum of IIA^{mtl} (3 mM, pH = 7.4) selectively enriched with [δ1,ε2-^{15}N]histidine. Our interpretation of the spectra in terms of the dominant tautomeric state of histidine residues A, B, and C is shown at the top of the figure.

Table II: Characterization of the Histidine Residues in IIA^{mtl} with Respect to Their ^{1}H Titration Parameters[a]

residue		IIA^{mtl}				$PIIA^{mtl}$			
		pK	δ_a (ppm)	δ_b (ppm)	$\Delta\delta$ (ppm)	pK	δ_a (ppm)	δ_b (ppm)	$\Delta\delta$ (ppm)
HisA	C2H	<5.80	7.58	n.o.		>8.50	n.o.	8.67	
	C4H	<5.80	6.82	n.o.		nd	n.o.	n.o.	
	Nδ1	<5.80	129	n.o.		nd	nd	nd	
	Nε2	<5.80	209	n.o.		nd	nd	nd	
HisB	C2H	7.30	7.75	8.72	0.97	7.46	7.72	8.67	0.95
	C4H	7.31	7.22	7.63	0.41	7.48	7.16	7.50	0.34
	Nδ1	7.32	201	169	32	nd	nd	nd	
	Nε2	7.30	203	178	25	nd	nd	nd	
HisC	C2H	6.58	7.62	8.64	1.07	7.15	7.71	8.14	0.43
	C4H	nd	6.88	6.92	0.04	nd	6.89	6.92	0.03
	Nδ1	nd	205	n.o.		nd	nd	nd	
	Nε2	nd	131	n.o.		nd	nd	nd	

[a] The parameters were obtained from the experimental data by a least-squares fitting procedure as is described in the text. n.o. = not observed; nd = not determined.

Apparently, the C4H experiences pH-dependent changes in its environment which influence its titration behavior.

^{15}N Titration Curves. HisA: The ^{15}N titration curve for HisA is shown in Figure 4. For reasons described in the previous section, the titration curve for this residue is incomplete. Consequently, the hydrogen bond structure at this residue can only be determined for the deprotonated imidazole ring. For this ring, two nitrogen resonances are observed, one at 129 ppm and one at 209 ppm. From the cross-peak pattern, Figure 2, it is clear that the proton is located at the Nε2 position. Neither nitrogen shows significant hydrogen bonding since they both resonate at positions which are very close to the ones expected for pure type α and β nuclei, 210 and 128 ppm, respectively.

HisB: This histidine shows an imidazole ring with a fast tautomerization in the neutral state. The titration curves are shown in Figure 4b. In the protonated state, both nitrogens resonate at high δ-values (201 and 203 ppm), indicating two type α^+ nitrogens not significantly involved in hydrogen bond formation. In the neutral imidazole ring, the Nδ1 is found at 169 ppm and the Nε2 at 178 ppm, the center between these two being at 174 ppm. The assignment of Nδ1 and Nε2 is based on the cross-peak intensity pattern. The C2H shows cross-peaks to both Nδ1 and Nε2; tautomerization will result in cross-peaks with more or less equal intensities, assuming that all nuclei show similar relaxation behaviors. The C4H shows a cross-peak to only Nε2; in a tautomeric equilibrium, the intensity of this cross-peak will be divided over two positions so that its intensity will always be lower than that of the corresponding C2H cross-peaks. The intensity of the C4H cross-peaks reflects the preferred protonation state of the Nε2 nucleus, which in HisB is the protonated state. This is reflected

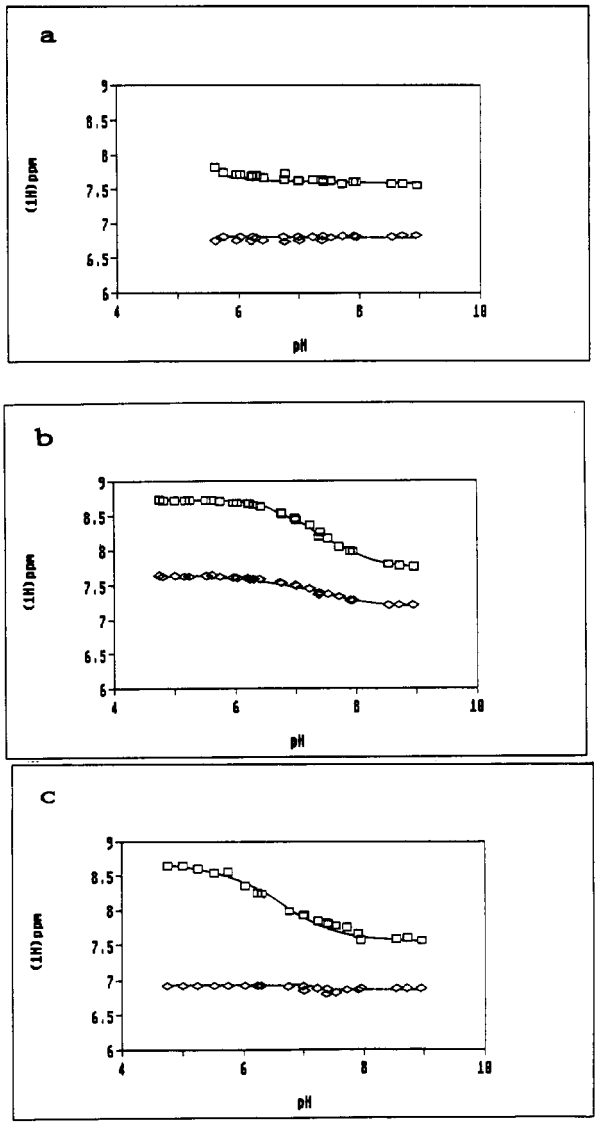

FIGURE 3: Titration curves for the histidine proton resonances in IIA^{mtl}. (a) HisA, (□) C2H, (◇) C4H; (b) HisB, (□) C2H, (◇) C4H; (c) HisC, (□) C2H, (◇) C4H. The points are the measured data. The solid line is the fit of these data points to eq 2, and the values derived from this fit are given in Table II.

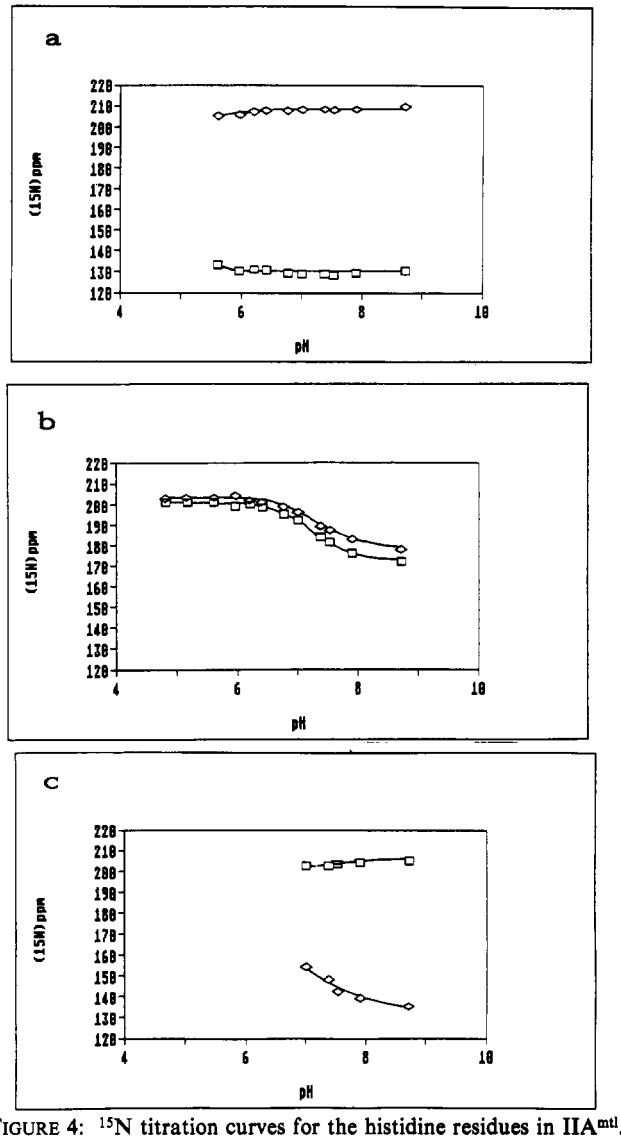

FIGURE 4: ^{15}N titration curves for the histidine residues in IIA^{mtl}. (a) HisA, (□) Nδ1, (◇) Nε2; (b) HisB, (□) Nδ1, (tso) Nε2; (c) HisC, (□) Nδ1, (◇) Nε2.

in the higher intensity of the cross-peak at a higher field (Figure 2). On the basis of the 9 ppm chemical shift difference between Nδ1 and Nε2, an equilibrium value (K = N(δ1)/N(ε2)) of 0.78 was calculated for the tautomeric process in the neutral imidazole ring. The calculation was performed as described in the previous section, using a δ-value for the β nucleus of 138 ppm instead of 128 ppm because of hydrogen bonding effects. Despite the rapid tautomerization, there is an indication that the neutral imidazole ring of HisB is hydrogen bonded. This can be derived from a center position of 174 ppm between Nδ1 and Nε2. If no hydrogen bond were present, this average position would be 169 ppm, the middle between the α-type and β-type nitrogen resonance positions. A higher average value means that either the α-type nitrogen resonance position has moved to values higher than 210 ppm or the β-type nitrogen position has moved to values higher than 128 ppm or that both positions have shifted to higher values. A higher value for the α-type nitrogen position cannot be explained in terms of H-bond formation. Hydrogen bonding would only move the resonance position to lower values (Table I). Hydrogen bond formation to a β-type nitrogen atom could, however, shift the resonance position from 128 to 138 ppm (Table I), and this value would explain the position of the center between Nδ1 and Nε2 at 174 ppm. This indicates that the deprotonated nitrogen of both tautomers is acting as a hydrogen bond acceptor. Such a situation requires that the hydrogen bond donating group be in close proximity to both imidazole nitrogens. This would be possible if the ring rotated rapidly so that the Nδ1 and Nε2 were pointing toward the H-bond donor. Rapid rotation is in agreement with the slow relaxation observed for this histidine. A fast tautomerization on the ^{15}N NMR time scale implies an exchange rate constant higher than about 1×10^5 s^{-1} (calculated using a chemical shift difference between the two nitrogens of 72 ppm). Rate constants of up to 10^9 s^{-1} have been reported for water molecules that were rather strongly hydrogen bonded to the deprotonated nitrogen in imidazole (Ralph & Grunwald, 1969). High exchange rates are also evidenced by the fact that the resonances of this histidine are observed over the complete titration range. Sudmeier et al. (1980) showed from theoretical considerations that the histidine nitrogen resonances are expected to broaden strongly during a titration at the high fields used in the present study. This should lead to the disappearance of the ^{15}N resonances from the NMR spectrum. The fact that the resonances are observed during the complete titration indicates that the exchange of protons

Table III: Characterization of the Hydrogen Bonding State of the Histidine Residues in IIA^{mtl} before Phosphorylation and Changes in the Hydrogen Bonding State upon Phosphorylation of IIA^{mtl}, Performed at pH = 8.1

a. Characterization before Phosphorylation

	neutral imidazole		protonated imidazole
HisA ($pK < 5.80$)	Nδ1	type β, no hydrogen bond	not observed
	Nε2	type α, no hydrogen bond	not observed
HisB ($pK = 7.30$)	Nδ1	fast tautomerization, proton preference for Nε2, strong	type α^+, no hydrogen bond
	Nε2	H bond to the β-type nitrogen	type α^+, no hydrogen bond
HisC ($pK = 6.58$)	Nδ1	type α, moderate hydrogen bond	not observed
	Nε2	type β, no hydrogen bond	not observed

b. Changes upon Phosphorylation

	not phosphorylated			phosphorylated		
HisA	$pK < 5.80$	Nδ1	no hydrogen bond	$pK > 8.50$	Nδ1	no hydrogen bond
		Nε2	no hydrogen bond		Nε2	phosphorylated
HisB	$pK = 7.30$	Nδ1	fast tautomerization,	$pK = 7.47$	Nδ1	fast tautomerization,
		Nε2	strong hydrogen bond		Nε2	no hydrogen bond
HisC	$pK = 6.70$	Nδ1	moderate hydrogen bond	$pK = 7.15$	Nδ1	no hydrogen bond
		Nε2	no hydrogen bond		Nε2	no hydrogen bond

is catalyzed. In the case of HisB, this can be done by the H-bond donating group at the imidazole ring or by buffer ions. Similar fast exchange equilibria have been reported before (Van Dijk et al., 1990).

HisC: Only a partial ^{15}N titration curve could be measured for this residue. (Figure 4c). Since the proton titration could be completely followed over the entire pH range and no significant line broadening was observed, the disappearance of the HMQC cross-peaks for HisC must be caused by line broadening of the nitrogen resonances. As just described, line broadening is expected for ^{15}N NMR titrations of histidine residues with normal protonation rates due to the 73 ppm titration range going from an α^+-type to β-type nitrogen (Sudmeier et al., 1980). However, these considerations do not explain the disappearance of the α^+- to α-type resonance unless very slow (de)protonation rates or an alteration in the tautomeric equilibrium as a function of pH is involved. Observation of the ^{15}N resonances at high pH only allows the hydrogen bond structure to be determined for the neutral imidazole ring. The Nδ1 resonates at 205 ppm, which is 5 ppm lower than expected for a pure type α nitrogen (Table I) and indicates the involvement of this nitrogen in a hydrogen bond of intermediate strength. The Nε2, resonating at 131 ppm, may be involved in weak hydrogen bond interactions, since it resonates 3 ppm higher than expected for a pure type β nitrogen (Table I). The hydrogen bond characterization is summarized in Table III, part a.

Alternative Conformation for One of the Histidine Residues

The HMQC spectrum of some preparations showed four instead of three histidine spin systems (see Figure 5). As there are only three histidines present in IIA^{mtl}, this must mean that one of the histidines occurs in two alternate states. The occurrence of two states for a histidine residue is not uncommon, and it has been described for the active site histidine in ribonuclease T1 (Schmidt et al., 1991) and for the histidine residues in HPr (Van Dijk et al., 1990). The "extra" histidine spin system has a protonated Nε2 nucleus and a deprotonated Nδ1 nucleus. The appearance of this extra spin system is accompanied by a decreased peak intensity of the C4H/Nε2 cross-peak of HisC (compare Figures 2 and 5). We will come back to this in the Discussion section.

^1H Titration Curves for the Histidine Residues in $PIIA^{mtl}$

One-dimensional ^1H NMR spectra of $PIIA^{mtl}$ were recorded at several pH values. The assignment of resonances to a particular histidine was done using the HMQC spectrum for $PIIA^{mtl}$ (Figure 6). The assignment of the histidines as HisA, HisB, or HisC was done by comparison with Figures 2 and 5, and by comparison of the ^1H titration data for IIA^{mtl} and $PIIA^{mtl}$. Similar cross-peak pattern in the HMQC spectrum combined with similarities in the pK_a values and proton chemical shifts led to the assignments, presented in Table II. The assignment of HisA is not straightforward from this comparison, but it will be discussed in the next section. The ^1H titration curves for $PIIA^{mtl}$ are given in Figure 7 and were analyzed as described previously by fitting to eq 2. The results are summarized in Table II. The most dramatic change is observed for HisA, whose pK_a is raised from below 5.8 to above 8.6. Above pH 8.6, the resonance of the C2H of HisA broadens and disappears from the 1D ^1H spectrum. The C4H resonance of this residue could not be unambiguously identified. The large change in pK_a, induced by the phosphorylation, make this residue the most likely candidate for the phosphorylation site, since active site histidine residues in other PTS proteins show similar changes upon phosphorylation. The conclusion will be confirmed by the HMQC spectrum of $PIIA^{mtl}$, to be discussed in the next section. HisB shows a small change in pK_a value (from 7.30 to 7.46); the proton titration behavior is almost the same as before the phosphorylation (Table II). HisC is more affected by the phosphorylation than HisB, but the changes are not as dramatic as for HisA. The pK_a is raised from 6.58 to 7.15 upon phosphorylation, and the total shift upon titration of the C2H is reduced from 1.07 to 0.43 ppm (Table I); the C4H titration is unchanged. These results indicate local changes in the surroundings of HisC when the protein becomes phosphorylated.

$^1H\{^{15}N\}$ HMQC Spectrum of $PIIA^{mtl}$

A pH of 8.1 was chosen for the HMQC spectrum for $PIIA^{mtl}$ (Figure 6) because the hydrolysis of the phosphoprotein is not too high at this pH, allowing for sufficient data acquisition. The phosphorylation of the protein was checked at several time intervals during the data acquisition by looking at characteristic frequencies in the resulting 2D spectra, indicating dephosphorylation.

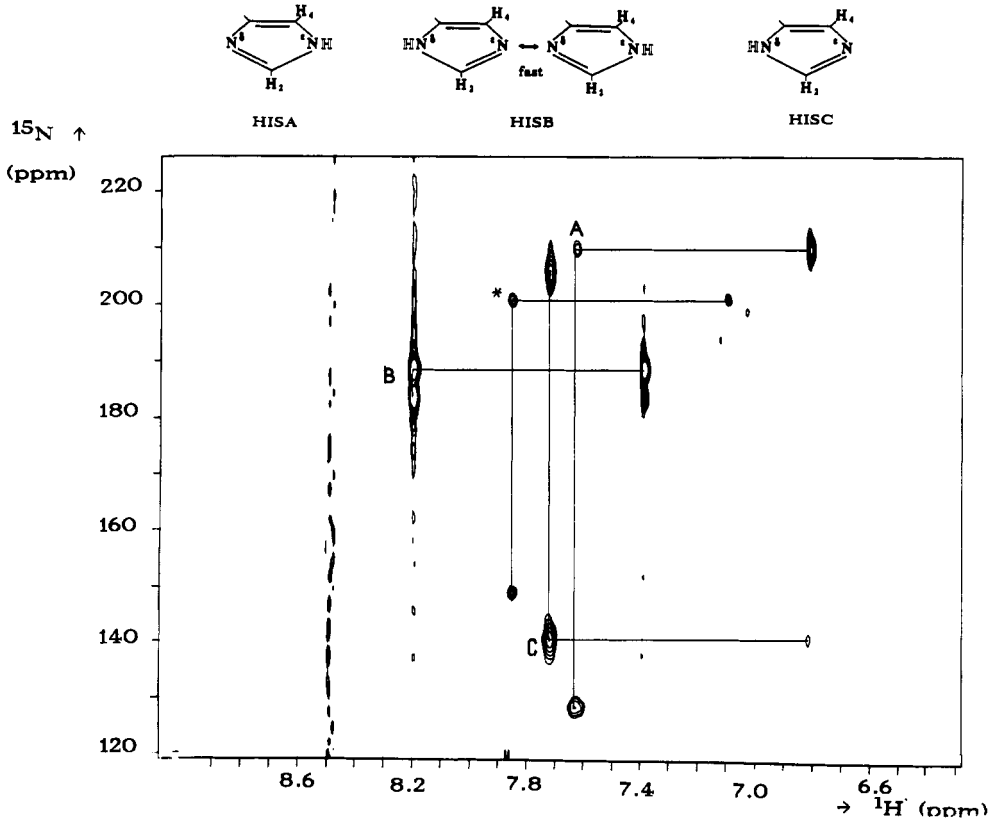

FIGURE 5: ^{1}H{^{15}N}HMQC spectrum of IIA^{mtl} (pH = 7.6) showing an alternative conformation of one of the histidine residues. The assignments of the histidine residues is the same as in Figure 3, HisA, HisB, and HisC having the same tautomeric state in both cases. The extra histidine spin system is indicated with an asterisk (*).

HisA: This residue is assigned as is indicated in Figure 6. No resonances are observed at the positions where HisA resonances occurred in the nonphosphorylated protein. The spin system, indicated in Figure 6 as HisA was also observed in the 1D ^{1}H NMR spectra. The Nδ1 resonance of this spin system is found at 202 ppm, indicative of an α^{+}-type nitrogen, or an α-type nitrogen, involved in strong H-bond formation. As the pK_a of this residue is above pK_a = 8.6 (Table II), the observed nitrogen obviously is α^{+}-type and is not involved in H-bond formation. The Nϵ2 of HisA is found at 166 ppm, a value typical for a phosphorylated imidazole nitrogen (Van Dijk et al., 1990). Because the Nϵ2 resonances are not intense in the contour plot, the ^{1}H trace at this ^{15}N frequency is plotted in Figure 6b, and the relevant resonances are indicated. The data thus indicate that HisA is the active site histidine and that phosphorylation takes place at the Nϵ2 position.

HisB: This residue was easily identified in the spectrum by its appearance and by its ^{1}H titration parameters, which are almost unaffected by the phosphorylation. A comparison of Figure 6 with Figures 2 and 5 shows, however, that the tautomeric equilibrium of this residue is affected by the phosphorylation process. Before phosphorylation, four resonances were observed for this residue, indicative of a fast tautomerization with the proton having a slight preference for the Nϵ2 position. In Figure 6 only two cross-peaks are observed for this residue at δ_{15N} = 175 ppm, one at each proton frequency. The peaks appear broad in the ^{15}N domain because the plost are contoured at low levels to detect the HisA and HisC cross-peaks. However, when the nitrogen trace at the C2H frequency is plotted, we clearly see only one resonance (Figure 6c). The HMQC spectrum of HisB in Figure 6a is analogous to the model spectrum in Figure 1b; they are both representative of a histidine showing a fast tautomerization with the proton being equally distributed over the two nitrogen positions. Furthermore, the resonance position at 175 ppm indicates that HisB is no longer hydrogen bonded. Calculations, using eq 2 and a pK_a of 7.47 for HisB in PIIA^{mtl} (Table II) give a theoretical chemical shift position of 175.1 ppm at pH = 8.1, the same as the observed resonance position. Before phosphorylation, there was a strong hydrogen bond at this residue which is apparently disturbed when the protein becomes phosphorylated.

HisC: The ^{1}H titration curves for this residue show that it is somewhat affected by the phosphorylation process (Table II). For clarity, we show the proton trace at the Nϵ2 frequency (133 ppm, Figure 6d) to indicate the expectation of the Nϵ2/C4H cross-peak, which is not observable at the contour level used in Figure 6a and only barely visible in Figure 5. This is the position found for the C4H in the nonphosphorylated protein (see Table II). The histidine still shows the same proton localization at the Nδ1 position, but its ^{15}N resonances at 206 and 133 ppm are at positions which are close to the ones calculated (204 and 134 ppm, respectively) for a non-hydrogen-bonded imidazole ring using the estimated pK_a for this residue (Table II). While there was a moderate hydrogen bond to the Nδ1 in IIA^{mtl}, phosphorylation disturbs the H-bond at HisC just as it did at HisB. The interpretations of the hydrogen bond changes are summarized in Table III, part b.

Remaining Cross-Peaks. It is clear from Figure 6 that more cross-peaks are present in the spectrum than expected. One of them is the "extra" spin system that was already observed in Figure 5 and which we interpreted as an alternative conformation of HisA, HisB, or HisC. Then, there remain some cross-peaks which all have a more or less diffuse appearance. They are found at positions that do not correspond with previously observed positions for HisA, HisB, or HisC. These cross-peaks may originate from IIA^{mtl} that cannot be properly phosphorylated. Gel filtration analysis showed the

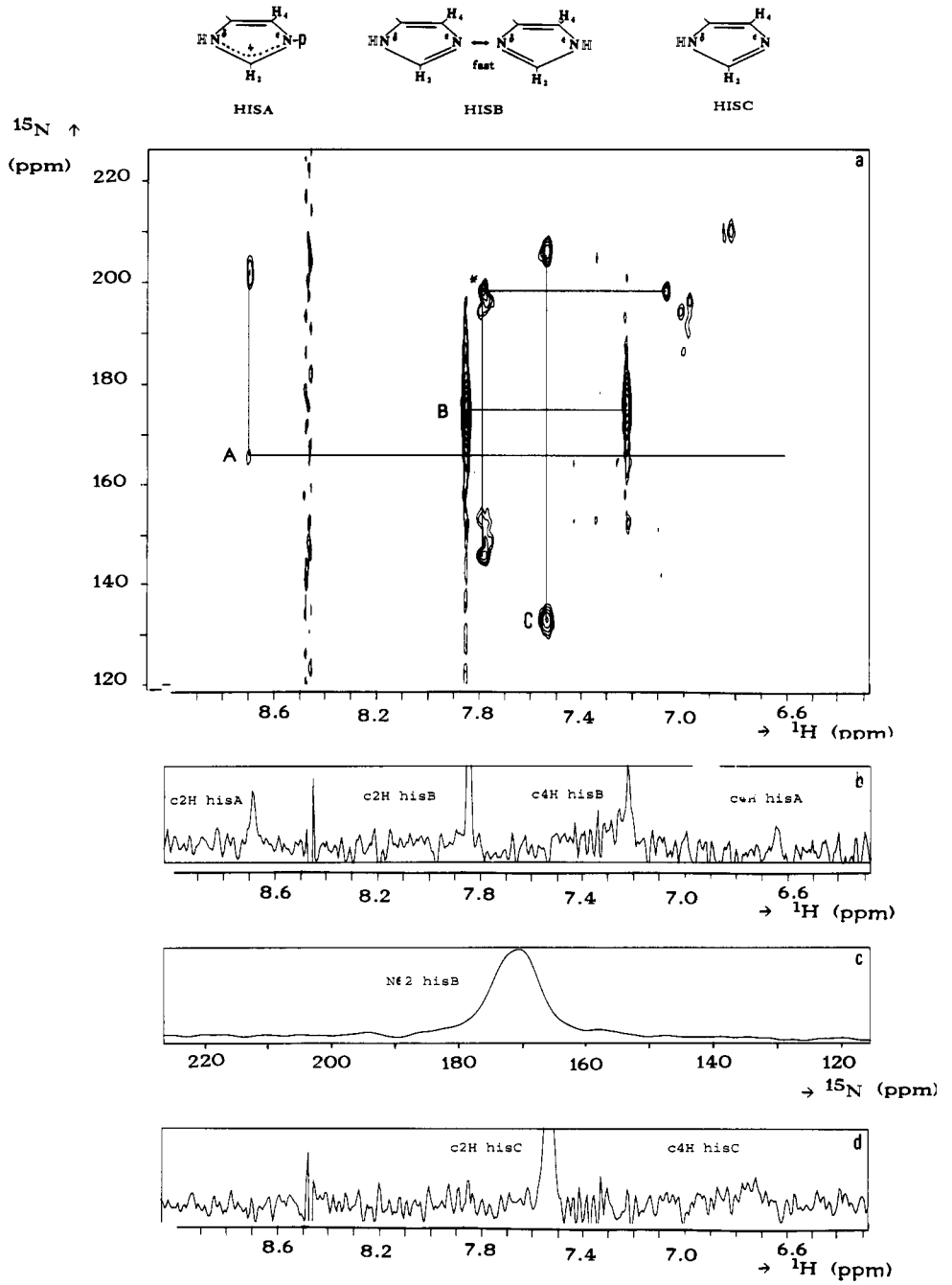

FIGURE 6: (a) $^{1}H\{^{15}\}$HMQC spectrum of PIIA. The dominant protonation state of the histidine residues is shown at the top of the figure. (b) Proton trace from panel a at δ_{15N} = 166 ppm. (c) Nitrogen trace from panel a at δ_{1H} = 7.87 ppm. (d) Proton trace from panel a at δ_{15N} = 133 ppm.

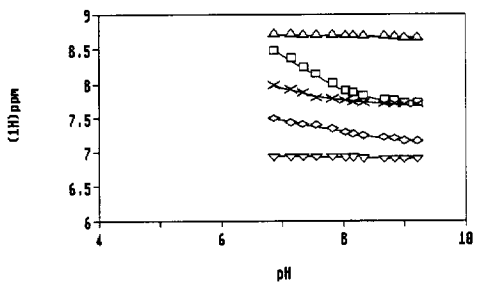

FIGURE 7: ^{1}H titration curves for the histidine residues in PIIA^{mtl}. Symbols: (△) C2H (HisA), (□) C2H (HisB), (◇) C4H (HisB), (×) C2H (HisC), (▽) C4H (HisC). The C4H of HisA could not be unambiguously identified.

presence of some dimeric and higher oligomeric forms of the protein which we showed to be inactive. At present, however, we cannot unambiguously explain the origin of the diffuse cross-peaks.

DISCUSSION

We have described the characterization of the three histidine residues in IIA^{mtl} with respect to their protonation state and their hydrogen-bonding interactions using 1D ^{1}H NMR and $^{1}H\{^{15}N\}$HMQC spectra. The ^{15}N-chemical shift data provide the information necessary to deduce the hydrogen bond interactions with the histidine imidazole rings. The data are summarized in Tables II and III. HisA proved to be the active site residue, and thus is equivalent to His554 in the intact EII^{mtl}. The phosphorylation takes place at the Nε2 position of the imidazole ring, which is analogous to that observed for other proteins with a function similar to that of IIA^{mtl} (Deutscher et al., 1982a; Dörschug et al., 1984). The

increase in pK_a of this residue upon phosphorylation is similar to what has been observed for the active site residues in other PTS proteins like HPr, IIA^{glc}, and IIA^{lac}, be it that the shift in the case of IIA^{mtl} is very large (from below 5.8 to above 8.6). There are several points to be stressed concerning the active site histidine. First, the imidazole ring is not hydrogen bonded in the phosphorylated or dephosphorylated state. Similar studies on HPr (Van Dijk et al., 1990) showed hydrogen bonding to the imidazole ring of the active site histidine that seemed to maintain the imidazole ring in a fixed position. The ring orientation was thought to be important for the phosphorylation of HPr, and we expected that a similar situation would occur in IIA^{mtl}. Second, there is a change in tautomeric state upon phosphorylation. The proton is situated at the Nϵ2 position in the nonphosphorylated protein (at pH > 5.8). This is also the place of attachment of the phosphoryl group. One would expect that the site of phosphorylation would be deprotonated so that the electrophilic phosphoryl group would be easily directed to the nucleophilic deprotonated imidazole nitrogen. This has been found for HPr (Van Dijk et al., 1990). After phosphorylation, the imidazole ring remains protonated as witnessed by its high pK_a (>8.6). Consequently, the proton shifts before or during the phosphorylation process from the Nϵ2 to the Nδ1 position. It is likely that the PHPr/IIA^{mtl} complex formed prior to phosphoryl transfer induces the change in the tautomeric state expected for an efficient phosphorylation reaction pathway. Evidence for such a PHPr/IIA^{mtl} complex has been found in ^{31}P NMR studies and will be reported elsewhere.

The phosphorylation process affects not only the active site residue, but also the other two histidine residues in IIA^{mtl}. Similar effects have been observed for the histidine residues in IIA^{lac} (Kalbitzer et al., 1981). Both are hydrogen bonded in the nonphosphorylated protein, but not in the phosphorylated IIA^{mtl}. Furthermore, changes in pK_a for both histidines and changes in the tautomerization state of HisB were observed, indicating that the phosphorylation induces overall conformational changes in the protein, a suggestion that is supported by the observation of a number of changes in the aliphatic region of the ^1H NMR spectrum (data not shown). In this respect, IIA^{mtl} behaves like IIA^{glc}, IIA^{xtl}, and IIA^{lac} which also show overall conformational changes upon phosphorylation (Dörschug et al., 1984; London & Hausman, 1983; Deutscher et al., 1982b). Our data suggest that one of the histidine residues experiences an alternative conformation. This has been assigned to HisC, since it is the only residue that shows a change in its relaxation behavior when the alternative histidine appears in the spectrum (compare Figures 2 and 5). High-resolution NMR studies are now in progress which will reveal the sequence assignments of HisB and HisC and hopefully provide a structural basis for understanding the significance, if any, of the alternative conformation observed for HisC.

The first high-resolution structures of IIA domains, IIA^{glc} from *Bacillus subtilis* and *Escherichia coli*, have recently been published (Liao et al., 1991; Worthylake et al., 1991). Since we expect IIA domains to function similarly, it is worth examining the data presented here in light of the X-ray structures of IIA^{glc}. It is essential to note, however, that there is no significant homology between the primary structures of IIA^{mtl} and the IIA^{glc} from either source. Furthermore, the tertiary structures of IIA^{mtl} will probably be very different from those of the IIA^{glc} since FTIR data in H_2O and D_2O show approximately 45% α-helix and 27% β-sheet for IIA^{mtl} from *E. coli* where both IIA^{glc} structures are dominated by β-sheet. The following comparison is based on the assumption that the arrangement of residues at the active site of IIA^{mtl} is similar to that of the two IIA^{glc} structures. The *B. subtilis* IIA^{glc} possesses two histidines in the active site region: His83 which becomes phosphorylated and His68. HisA in IIA^{mtl} corresponds to His83. Since HisB appears to be situated on the exterior of the protein and since HisC is more strongly affected by the phosphorylation, HisC probably corresponds to His68. Both *B. subtilis* IIA^{glc} histidines are associated with phenylalanine residues, and these are thought to be important for the relative orientation of the two histidine imidazole rings; no clear hydrogen bonds at the imidazole rings have been observed, although Liao et al. (1991) point out that there are indications for the presence of such structures. The absence of hydrogen bonds at the active site His83 in IIA^{glc} would be similar to what we observed for the HisA in IIA^{mtl}. Furthermore, the presence of a phenylalanine near HisC, the other suggested histidine in the active site of IIA^{mtl}, could explain the abnormally small pH-dependent shift of the C4H of this residue. A change in ring current shift due to movement of the two residues relative to one another upon (de)protonation is all that is necessary. In their model of the phosphorylated IIA^{glc}, Liao et al. (1991) suggest that the phosphoryl oxygen atoms would interact with the Nϵ2 of His68 while the Nδ1 of this residue would hydrogen bond to a side chain oxygen of a threonine residue. This is contrary to our finding that neither nitrogen atom of HisC in IIA^{mtl} is hydrogen bonded in the phosphorylated enzyme. The weak intensity of the Nϵ2/C4H cross-peak for HisC in IIA^{mtl} may arise from intermediate exchange dynamics with other species or intermediates which we cannot detect. Finally, the Nϵ2 of HisC is a β-type nitrogen (i.e., not protonated) and not able to serve as a H-bond donor to the phosphoryl oxygens.

In the case of IIA^{glc} from *E. coli*, Worthylake et al. (1991) report that the Nδ1 nitrogens of both histidines at the active site are hydrogen bonded; that of His90, the phosphorylation site, to the carbonyl oxygen of Gly92 (2.7 Å) and that of His71 to Oγ1 of Thr73 (3.1 Å). His90 would correspond to our HisA. As summarized in part a of Table III, the Nδ1 of HisA is not protonated at neutral pH, in contrast to the His90 Nδ1 in IIA^{glc}, and it is not involved in hydrogen bond formation. The Nδ1 of HisC which may correspond to His71 is hydrogen bonded.

In conclusion, there are some similarities between the proposals for the active site configuration arising from the X-ray data for IIA^{glc} from *B. subtilis* or *E. coli* and the NMR data for IIA^{mtl} from *E. coli* in the unphosphorylated enzymes, but there is not full agreement. Furthermore, the proposals for the phosphorylated domains of *E. coli* IIA^{mtl} versus those of *B. subtilis* IIA^{glc} differ significantly. All of these differences may reflect differences in the atomic details at the phosphorylation sites of the three enzymes if not differences in phosphorylation mechanism itself.

Presper et al. (1989) proposed a possible role for a second histidine as a migration site from the phosphoryl group on its way to the IIB domain. The finding, in both crystal structures, of two histidines with their ϵ2 nitrogens close enough together to accommodate such a transition is enticing. But again, the present NMR data do not support such a proposal for IIA^{mtl}; phosphorylation dramatically affects only one histidine, HisA. Neither of the other two histidines is that strongly affected. It is possible, however, that such a migration will only occur when stoichiometric amounts of PHPr or the B domain are present. Experiments are in progress to test these suggestions.

REFERENCES

Bachovchin, W. W. (1985) *Proc. Natl. Acad. Sci. U.S.A. 82*, 7948–7951.

Bachovchin, W. W. (1986) *Biochemistry 25*, 7751–7759.

Bachovchin, W. W., & Roberts, J. D. (1978) *J. Am. Chem. Soc. 100*, 8041–8047.

Bendall, M. R., Pegg, D. T., & Doddrell, D. M. (1983) *J. Magn. Reson. 52*, 81–117.

Blomberg, F., Maurer, H., & Rüterjans, H. (1977) *J. Am. Chem. Soc. 99*, 8149–8159.

Deutscher, J., Beyreuther, K., Sobek, H. M., Stüber, K., & Hengstenberg, W. (1982a) *Biochemistry 20*, 6178–6185.

Deutscher, J., Beyreuther, K., Sobek, H. M., Stüber, K., & Hengstenberg, W. (1982b) *Biochemistry 21*, 4867–4873.

Dörschug, M., Frank, R., Kalbitzer, H. R., Hengstenberg, W., & Deutscher, J. (1984) *Eur. J. Biochem. 144*, 113–119.

Ernst, R. R., Bodenhausen, G., & Wokaun, A. (1987) *Principles of nuclear magnetic resonance in one and two dimensions*, Oxford University Press, New York.

Kalbitzer, H. R., Deutscher, J., Hengstenberg, W., & Rösch, P. (1981) *Biochemistry 21*, 6178–6185.

London, J., & Hausman, S. Z. (1983) *J. Bacteriol. 156*, 329–340.

Liao, D.-I., Kapadia, G., Reddy, P., Saier, M. H., Jr., Reizer, J., & Herzberg, O. (1991) *Biochemistry 30*, 9583–9594.

Pas, H. H., & Robillard, G. T. (1988) *Biochemistry 27*, 5835–5839.

Pas, H. H., Ten Hoeve-Duurkens, R. H., & Robillard, G. T. (1988) *Biochemistry 27*, 5520–5525.

Pas, H. H., Meyer, G., Kruizinga, W. H., Tamminga, K. S., Van Weeghel, R. P., & Robillard, G. T. (1991) *J. Biol. Chem. 266*, 6690–6692.

Presper, K. A., Wong, C.-Y., Liu, L., Meadow, N. D., & Roseman, S. (1989) *Proc. Natl. Acad. Sci. U.S.A. 86*, 4052–4055.

Ralphe, E. K., & Grunwald, E. (1969) *J. Am. Chem. Soc. 91*, 2422–2425.

Robillard, G. T., Dooijewaard, G., & Lolkema, J. (1979) *Biochemistry 18*, 2948–2989.

Robillard, G. T., & Blaauw, M. (1987) *Biochemistry 26*, 5796–5803.

Saier, M. H., Jr., & Reizer, J. (1991) *Res. Microbiol. 141*, 1033–1038.

Schmidt, J. M., Thüring, H., Werner, A., Rüterjans, H., Quaas, R., & Hahn, U. (1991) *Eur. J. Biochem. 197*, 643–653.

Soerensen, O. W., Eich, G. W., Levitt, M. H., Bodenhausen, G., & Ernst, R. R. (1983) *Prog. Nucl. Magn. Reson. Spectrosc. 16*, 163–192.

Sudmeier, J. L., Evelhoch, J. L., & Jonsson, N. B. H. (1980) *J. Magn. Reson. 40*, 377–390.

Van Dijk, A. A., De Lange, L. C. M., Bachovchin, W. W., & Robillard, G. T. (1990) *Biochemistry 29*, 8164–8171.

Van Weeghel, R. P., Meyer, G., Keck, W. H., & Robillard, G. T. (1991) *Biochemistry 30*, 1774–1779.

Worthylake, D., Meadow, N. D., Roseman, S., Liao, D., Herzberg, O., & Remington, S. T. (1991) *Proc. Natl. Acad. Sci. U.S.A. 88*, 10382–10386.

Registry No. His, 71-00-1.